**Highlights:**

- A complete photoemission (XPS, UPS, IPES) and X-ray adsorption (NEXAFS) analysis of single- and multilayer Co-TPP films on the Fe(001)-*p*(1 × 1)O substrate.

- A commensurate superstructure is observed by electron diffraction when Co-TPP molecules are grown on the Fe(001)-*p*(1 × 1)O substrate.

- NEXAFS and photoemission suggest that the Co-TPP/substrate interaction is localized on the Co(II) ion.

# Cobalt atoms drive the anchoring of Co-TPP molecules to the oxygen-passivated Fe(001) surface

A. Calloni[1], M.S. Jagadeesh[1], G. Bussetti[1*], G. Fratesi[2], S. Achilli[3], A. Picone[1], A. Lodesani[1], A. Brambilla[1], C. Goletti[4], F. Ciccacci[1], L. Duò[1], M. Finazzi[1], A. Goldoni[5], A. Verdini[6], L. Floreano[6]

[1] *Department of Physics, Politecnico di Milano, p.za Leonardo da Vinci 32, I-20133 Milano, Italy*
[2] *ETSF and Dipartimento di Fisica, Università degli Studi di Milano, Via Celoria, 16, 20133 Milano, Italy*
[3] *Catalan Institute of Nanoscience and Nanotechnology, Av. de Serragalliners, 08193 Bellaterra Barcelona, Spain*
[4] *Dipartimento di Fisica, Università di Roma 'Tor Vergata', via della Ricerca Scientifica, 1, 00133 Roma, Italy*
[5] *Elettra Sincrotrone Trieste, s.s. 14 km 163.5 in Area Science Park, 34149 Trieste, Italy*
[6] *Istituto Officina dei Materiali – CNR-IOM, Laboratorio TASC s.s 14 km 163.5, 34149 Trieste, Italy*

* e-mail: gianlorenzo.bussetti@polimi.it

## Abstract:

We present a multitechnique investigation of the structural and electronic properties of the prototypical system composed by ultra-thin films of magnetic molecules [Co-tetraphenyl-porphyrins (Co-TPP)] grown on a ferromagnetic substrate [oxygen passivated Fe(001), namely the Fe(001)-*p*(1 × 1)O surface]. Low Energy electron diffraction (LEED) and scanning tunneling microscopy (STM), coupled with first-principles calculations, reveal the formation of a commensurate superstructure at monolayer coverage, made by a square array of flat-lying TPP molecules. UV-photoemission and inverse photoemission spectroscopies (UPS and IPES) are used to investigate their electronic structure. Similar to our previous results on the Zn-TPP growth on Fe(001)-*p*(1 × 1)O, the passivation of the metallic surface is able to preserve the photoemission features characteristic of quasi-free molecules, opening the route towards an exploitation of single oxide layers as protective films in organic/inorganic junctions. X-ray photoemission (XPS) and near edge X-ray adsorption fine structure spectroscopies (NEXAFS), are used to reveal the details of the Co-TPP interaction with the substrate.

**Keywords:** Co-TPP, Fe(001)-*p*(1×1)O, ultra-thin metal-oxide interface, photoemission, IPES, NEXAFS.

## 1. Introduction

Metal tetraphenyl porphyrins (M-TPP) are an interesting class of organic molecules characterized by a ring-like planar structure with an inner cavity (the tetra-pyrrole ring) surrounded by four phenyl groups, which are free to tilt with respect to the molecular plane. A metal ion is located at the center of the cavity, giving unique physical-chemical characteristics to the compound, widely exploited in nature *e.g.*, in catalytic and biological processes [1–3].

M-TPP can be sublimated in a ultra-high vacuum (UHV) environment by means of effusion crucibles (Knudsen cells) at very low molecular rates [4,5]. The resulting thin and ultra-thin organic films are characterized by a high chemical purity and structural quality [6], which are mandatory in the perspective realization of devices exploiting TPP molecules. Due to its open structure, the tetra-pyrrole ring can be strongly perturbed by the environment (gases, surface). This perturbation has a direct effect on the TPP electronic and transport properties (both in-plane and out-of-plane), since those states involved in electrical conduction are localized on the ring. An important research effort is aimed, for instance, at the ring protection when porphyrins lie flat on a substrate, as in ultrathin films. In these conditions, the molecule-substrate interaction should be minimized [6]. A viable strategy is to choose organic crystals [7], graphite [8] or low-interacting metals, such as Au [9]. Conversely, magnetic substrates could represent interesting platforms for driving specific interactions with Co- [10], Ni- [11] or Fe-TPP [12] molecules. For semiconductor [13] or metal [14] substrates, surface passivation is a way to preserve the molecular properties. A possible strategy in this direction is the use of thick and thin metal-oxide films [15,16] or even ultra-thin metal-oxide films. A prototypical system belonging to the last category is the Fe(001)-$p(1 \times 1)$O surface, where a single layer of oxygen atoms fills the hollow sites of the (001) iron surface [14]. The authors have checked the adequacy of this surface by using Zn-TPP molecules, proving that (i) the oxide layer is stable after subsequent TPP depositions, and (ii) porphyrins retain a certain mobility, allowing for the

formation of a commensurate square-lattice superstructure when the first layer is completed [14]. This opens the route towards the growth of ordered assembly of molecules onto a magnetic substrate for applications in organic spintronics. In this respect, the Fe(001)-*p*(1 × 1)O is of particular interest due to the observed high spin polarization [17].

In this work, we investigate the assembling and the electronic properties of Co-TPP films with a thickness variable from fractions of a single molecular layer, to a monolayer (ML) and to several layers (up to 4 ML). This is done by employing a variety of surface science techniques such as scanning tunneling microscopy (STM), supported by first-principles calculations, low-energy electron diffraction (LEED), X-ray and UV photoemission spectroscopy (XPS and UPS, respectively), inverse photoemission spectroscopy (IPES) and near edge X-ray adsorption fine structure (NEXAFS).

STM, LEED and NEXAFS (performed at the K edges of C and N), together with first-principles calculations, give a detailed picture of the surface morphology and molecular conformation. According to our results, Co-TPP molecules lie flat on the Fe-*p*(1 × 1)O surface and arrange to form a commensurate square lattice as in the case of Zn-TPP, but rotated by $\pm\theta$ (with $\theta = 37\,°$) with respect to the [100] substrate crystallographic directions. UPS and IPES show that the Co-TPP occupied and empty states are preserved also at ML coverage, with few differences with respect to free-standing molecules (*i.e.* those embedded in thicker layers), related to the interaction with the substrate. By combining the results coming from XPS, NEXAFS performed at the Co $L_{2,3}$-edges, we localize the molecule-substrate interaction on the molecular ring, and in particular on the Co ion.

## 2. Materials and methods

The Fe(001)-*p*(1 × 1)O substrate was prepared following a procedure reported in the literature [18,19]. The clean Fe substrate is exposed to few langmuir of molecular oxygen (grade 5.5) and then it is annealed at about 700 °C. Knudsen effusion cells sublimated porphyrins at around 300 °C. The deposition flux was 0.5 ML/min, being 1 ML = 3.06 Å [13], as monitored by a quartz microbalance. The spectra acquired on the thick (4 ML) film highlight the main spectroscopic features of Co-TPP molecules. XPS and UPS were performed at $h\nu$ = 1253.6 eV (Mg Kα radiation) and at $h\nu$ = 21.2 eV radiation (HeI radiation), respectively. A GaAs(001) photocathode, prepared following standard procedures reported in the literature [20,21], was employed to provide electrons for IPES. The IPES setup was operated in isochromatic mode, *i.e.* by changing the energy of the impinging electrons and detecting 9.6 eV inverse photoemission photons with a band-pass detector [22–24]. The full width at half maximum (FWHM) energy resolution of XPS, UPS and IPES is about 0.9 eV, $15 \cdot 10^{-3}$ eV and 0.7 eV, respectively. The UPS (IPES) analysis was performed by collecting (sending) the electrons at normal emission (incidence). All the experiments reported here were performed at room temperature under negligible charging conditions during electron spectroscopy data acquisition. The position of the vacuum level was obtained from the low-energy secondary electron cutoff acquired by applying a negative bias to the sample (−10 V).

NEXAFS spectra were acquired at the ALOISA beamline at the Elettra synchrotron radiation facility (Trieste, Italy), in partial electron yield mode by means of a channeltron equipped with a negatively biased grid to filter out low energy secondary electrons and increase the signal to background ratio. To investigate the sample dichroism, spectra have been collected with the surface oriented either parallel to the electric field (*s*-polarization) or closely normal to it (*p*-polarization), while the light grazing angle was kept constant at 6°. The photon flux normalization and the

energy calibration are described elsewhere [25]. The photon energy resolution was set to $80 \cdot 10^{-3}$ eV.

STM images were collected at room temperature in the constant-current mode by using home-made etched W tips. The latter were introduced in vacuum without any annealing. The sample was grounded, thus positive bias applied to the tips correspond to tunneling from filled molecular states.

First-principles calculations were performed in the framework of density functional theory (DFT). The exchange-correlation was approximated by the vdW-DF-c09 functional [26] that includes dispersion forces. All simulations have been performed with the Quantum-ESPRESSO package [27, 28] that implements ultrasoft pseudopotentials and plane waves. Pseudopotentials were generated starting from scalar-relativistic all-electron calculations and using non-linear core corrections.

A slab model of the Fe(001)-*p*(1 × 1)O surface was adopted, in analogy to our previous works,[29] having O adsorbed on the top side of the slab and the bottom two Fe layers (out of four) fixed at bulk interlayer distances. The periodic replicas of the slab are separated by a vacuum space of about 17 Å. A square surface unit cell with the $\begin{pmatrix} 4 & 3 \\ -3 & 4 \end{pmatrix}$ periodicity is constructed, as observed in the LEED experiments presented below. The Brillouin zone is sampled by a shifted Monkhorst-Pack [30] 2×2 grid. Molecules are then placed on the top surface and their coordinates optimized until the forces on atoms are lower than 0.1 mRy/Bohr, an order of magnitude smaller than the default to handle the mild dependence of energy on structural details, especially concerning the phenyl coordinates.

To treat on-site correlation at the Co atom, we make use of the DFT+U approach in the rotationally-invariant form with a single parameter $U_{\text{eff}} = U - J = 3.0$ eV, having chosen $U = 4.0$ eV and $J = 1.0$ eV as proposed in several works [31-33]. This value produces orbital order for free Co-TPP in close agreement to reference works [34]. Neglecting the "+U" correction instead results in a very low-energy spin-minority $d_{z^2}$ state, becoming the LUMO of gas phase Co-TPP instead of states located on the tetra-

pyrrole macrocycle. We remark that full structural relaxations performed without the "+U" corrections gave very similar optimized coordinates.

## 3. Results and Discussion

### 3.1. *LEED and STM characterizations*.

**Figure 1** shows the diffraction patterns observed (a) on the bare substrate and (b) after the deposition of 1 ML of Co-TPP molecules. The Co-TPP pattern can be attributed to the presence of a commensurate superstructure described in the reciprocal space by the matrix $\begin{pmatrix} 4 & 3 \\ -3 & 4 \end{pmatrix}$ and its mirror $\begin{pmatrix} 4 & -3 \\ -3 & -4 \end{pmatrix}$, as clarified by a simulation made with the LEEDpat4 software [35] and shown in (c). In real space, this translates into the presence of two different domains featuring square molecular lattices rotated by $\pm\,\theta$ with respect to the substrate [100] direction. The molecule-molecule distance is 5 iron lattice-steps, in analogy with the inter-molecular spacing observed for the Zn-TPP superstructure [36].

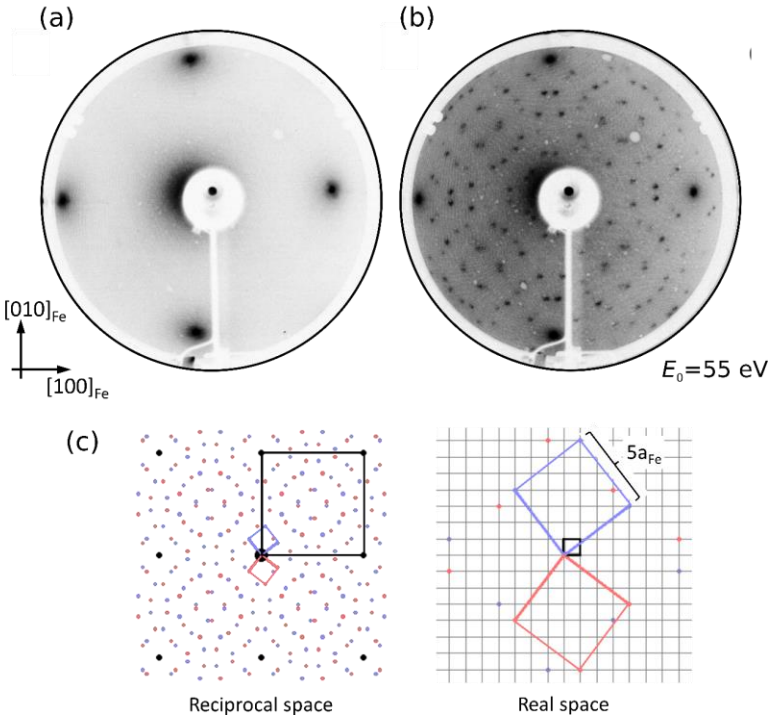


**Figure 1.** LEED patterns acquired with an electron beam energy of 55 eV on (a) Fe(001)-*p*(1 × 1)O and (b) 1 ML Co-TPP/Fe(001)-*p*(1 × 1)O. (c) LEED pattern analysis performed with the LEEDpat4 software [35], showing the reciprocal space pattern (left) and the real space (right) superstructure. Black squares are representative of the Fe(001) surface unit cell, while violet and pink ones are related to the two equivalent domains of the molecular superstructure (see the text for details).

Interestingly, despite having the same peripheral structure, Co-TPP molecules create a different molecular arrangement on the substrate with respect to Zn-TPP, the latter forming a *p*(5 × 5) superstructure. This difference is likely due to the different metal ion. The Zn ion radius is slightly larger (about 10 %) than that of Co, suggesting that the molecular skeleton is reasonably affected by different transition metals placed inside the tetra-pyrrole cavity.

In **Figure 2**, it is possible to appreciate that the fourfold symmetry characteristic of the free molecule is preserved upon adsorption on the Fe(001)-*p*(1 × 1)O substrate.

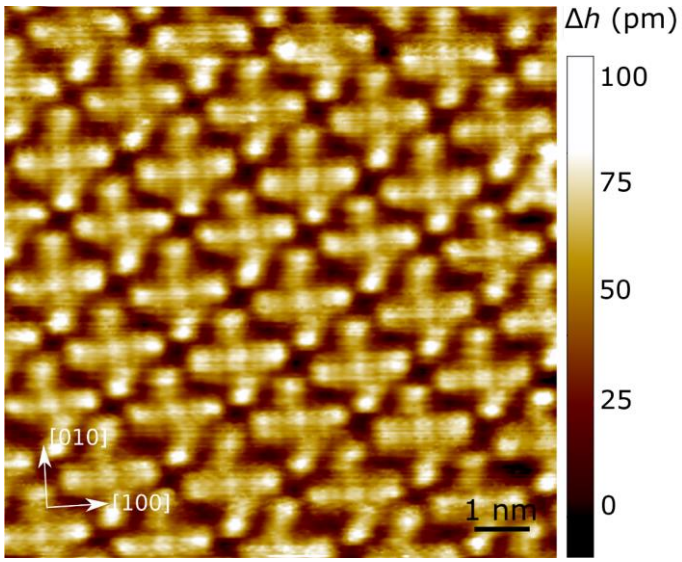


**Figure 2.** Close up view of the surface showing the molecular packing of the Co-TPP wetting layer deposited on Fe(001)-*p*(1 × 1)O substrate. The image size is 10 × 10 nm$^2$, tunneling parameters are $V$ = 2 V and $I$ = 1 nA. The color bars indicate the relative topographic height for the corresponding images. The crystallographic axis refer to the substrate.

3.2 *Photoemission characterization*.

UPS and IPES spectra acquired on Co-TPP at the coverages of 1 ML and 4 ML, together with reference spectra from the substrate, are shown in **Figure 3**.

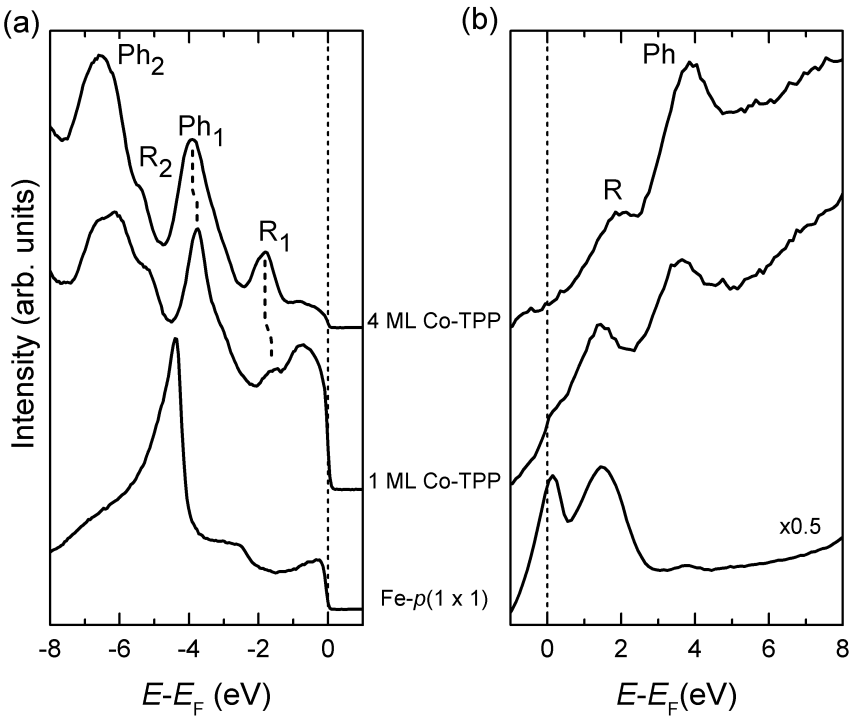


**Figure 3.** (a) photoemission and (b) inverse photoemission results for two Co-TPP coverages (namely 1 ML and 4 ML). The spectra related to Fe(001)-*p*(1 × 1)O substrate are added for comparison. Labels "R" or "Ph" are related to photoemission from either the tetra-pyrrole ring or the phenyl groups, respectively.

The 4 ML UPS spectrum is characterized by four peaks, arising from states located either in the tetra-pyrrole ring (R) or in the phenyl groups (Ph). They are labelled with a number (1 or 2) according to theoretical calculations of TPP molecules [13, 37]. The lower spectral resolution of IPES does not allow a fine identification of empty states as for filled ones. Nonetheless, the closer feature to the Fermi level is identified as the ring LUMO level while the second peak is interpreted in terms of phenyl groups contribution to the LUMO states [37].

The valence band characterization of the ultra-thin (1 ML) film reveals all the features of the molecules (namely, $R_{1,2}$ and $Ph_{1,2}$), suggesting that the buried oxygen layer has preserved their electronic structure, as also observed in our previous study on the Zn-TPP/Fe(001)-*p*(1 × 1)O system [36]. **Figure 4** shows a close-up of Co-TPP valence states located in close proximity to $E_F$ and contributing to feature $R_1$. The experimental results from Zn-TPP molecules are added here for comparison. In view

of enhancing the Co-TPP features close to the Fermi level, the contribution from the Fe(001)-*p*(1×1)O substrate (highlighted with a dashed line) was subtracted.

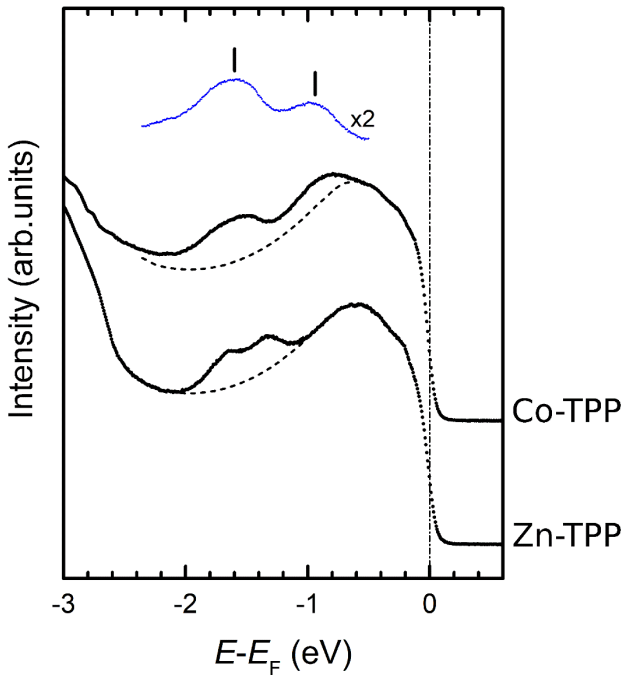


**Figure 4.** Close-up of the valence electronic structure of 1ML of M-TPP (M = Co, Zn). Dashed lines are representative of the photoemission intensity from the substrate. Blue dots: difference spectra (Co-TPP baseline) highlighting the contribution of molecular orbitals in the Co-TPP spectrum.

Feature $R_1$ in the Zn-TPP spectrum is the sum of two peaks located at about -1.3 eV and -1.7 eV, in agreement with the splitting observed in more resolved gas-phase photoemission spectra [38]. Since Zn-TPP molecules are characterized by a completely filled *d* shell, the contribution of Zn ions to the states at the Fermi level is negligible and the HOMO features can be related to ligand states.

The Co-TPP spectrum is characterized by a broad feature peaking at about -1.6 eV, visible also on the thick film and consistent with the experimental results shown in Ref. [39]. This feature is located at about the same energy of the Zn-TPP one, suggesting a contribution from ligand states. However, some authors observe a contribution from Co *d* states in the same energy region [40]. Another feature, located at an energy of about -0.95 eV, is highlighted by subtracting the Fe(001)-*p*(1×1)O

contribution (**Figure 4,** blue dots spectrum). Since the relative intensity of this feature is almost nil on the thick film (see **Figure 3**), we relate it to photoemission from electronic states located in the first Co-TPP ML or at the Co-TPP/substrate interface.

At variance with Zn-TPP, Co-TPP molecules are characterized (in their free state) by an incomplete *3d* shell [41]: a contribution from electronic states related to the inner metal ion is therefore expected. As will be further discussed in the following, the appearance of the -0.95 eV peak can be linked to the filling of Co 3*d* states due to molecular hybridization with the substrate, in analogy with the literature results for the Co-TPP/ Ag(111) system [40,42].

**Table 1** reports the energy positions of the HOMO ($R_1$, $Ph_1$) and LUMO (R, Ph) features. The value in brackets is related to the energy position of the peak close to $E_F$ detected at 1 ML coverage. At the same coverage, the R LUMO feature overlaps with the photoemission signal from the substrate. Its position was therefore determined by evaluating the position of the Ph LUMO feature and assuming the same R-Ph energy difference observed on the 4 ML film, as confirmed by comparing the homologous $R_1$-$Ph_1$ energy differences of the filled states. The photoemission features clearly shift towards the Fermi energy ($E_F$) by moving from the thick to the ultra-thin film. This is likely related to a more efficient screening of the photogenerated hole (added electron for IPES) on the ultra-thin film, in analogy with our previous results obtained for the growth of $C_{60}$ molecules on Fe(001)-$p$(1 × 1)O [43].

| | **1 ML thick sample** | **4 ML thick sample** |
|---|---|---|
| $R_1$ HOMO | -1.58(0.95) ± 0.05 eV | -1.78 ± 0.05 eV |
| $Ph_1$ HOMO | -3.77 ± 0.05 eV | -3.93 ± 0.05 eV |
| R LUMO | 1.5 ± 0.3 eV | 1.7 ± 0.3 eV |
| Ph LUMO | 3.5 ± 0.3 eV | 3.7 ± 0.3 eV |

**Table 1.** Energy positions with respect to the Fermi level of the photoemission features from the Co-TPP films of Figures 3 and 4. The value reported within brackets is related to the UPS feature observed close to $E_F$ on the 1 ML film.

The HOMO-LUMO energy gap ($E_G$) can be determined by considering the leading edges of the HOMO $R_1$ feature and the peak position of the LUMO R, in order to account for the lower energy resolution of IPES (see **Figure S1** of the Supplemental Information). We measure an $E_G$ of about 3.0 ± 0.3 eV for the thick film. This result is in agreement with the Co-TPP optical gap of 2.3 eV reported in the literature [44], considering that the molecular exciton binding energy is usually of several hundreds of meV [45]. $E_G$ reduces to 2.1 ± 0.3 eV in the ML film, accounting for the different way Co-TPP electronic states are populated (*i.e.* by considering the -0.95 eV feature of **Figure 4**).

XPS results for the (a) N 1*s* and (b) Co 2$p_{3/2}$ spectral regions are shown in **Figure 5**.

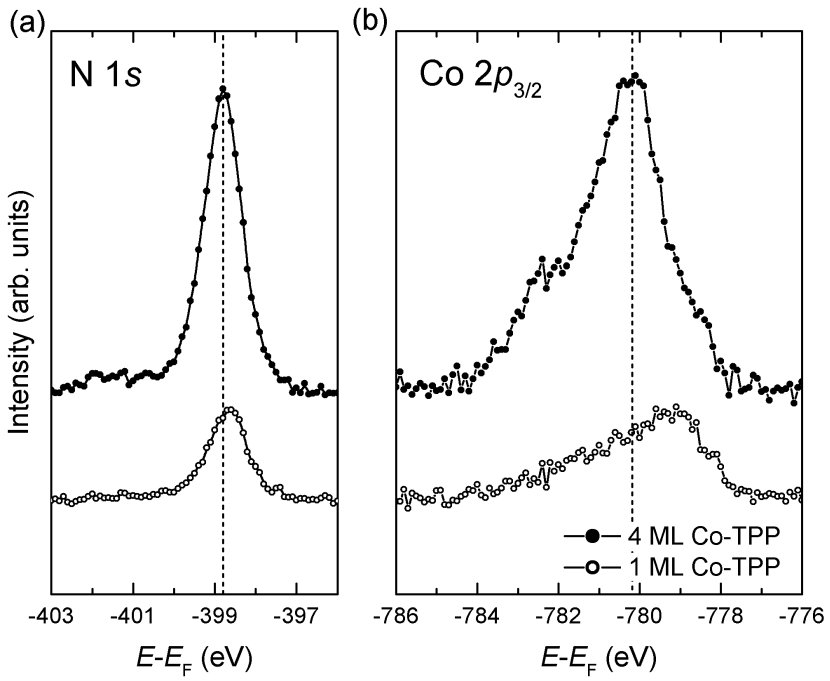


**Figure 5.** XPS spectra related to 1 ML and multilayer (4 ML) films of Co-TPP/Fe(001)-*p*(1 × 1)O showing (a) the N 1*s* and (b) the Co 2$p_{3/2}$ spectral regions. All spectra are plotted after the subtraction of a linear background.

The energy positions of the N 1*s* and Co 2$p_{3/2}$ peaks in the 4 ML Co-TPP film are in agreement with the values reported in the literature for thick films of Co-TPP molecules [36]. The photoemission spectrum from the Co 2$p_{3/2}$ orbital, showing a main feature at an energy of -780.2 eV (typical of photoemission from Co(II) ions [46]), is

characterized by a multiplet lineshape due to the coupling of the Co core hole created during photoemission with the unpaired electron in the Co outer shell [40].

The Co $2p_{3/2}$ peak from the 1 ML Co-TPP show a significantly different lineshape. It is still characterized by an asymmetric tail extending towards larger binding energies, possibly hiding a multiplet structure as for the thick film. The maximum intensity is reached at an energy of -779.2 eV, 1.0 eV away from the centroid of the main feature recorded on the thick film. We disregard the hypothesis of a screening effect, since the energy shift observed in the photoemission spectra from other elements (see *e.g.* the results from the N ligands) is much smaller than this value. The observed shift is most likely related to charge transfer from the substrate to the Co ion, associated with the population of molecular electronic states close to $E_F$, as observed with UPS. Similar findings are reported in the literature for the monolayer phase of Co-TPP/Ag(111) [40,42] and NiTPP/Cu(100) [47], however both systems yield a 1.7-1.8 eV shift of the corresponding $2p_{3/2}$ peak. Such a large core level shift indicates an effective reduction of the oxidation state of the central metal due to the substrate charge transfer. The lower shift observed in the present case might be related to the passivating action of the interfacial Fe oxide layer.

### 3.3 *NEXAFS characterization*.

**Figure 6**a(b) shows the NEXAFS spectra acquired at the N(C) K-edge on Co-TPP ML and multilayer (4 ML) films. Each set of spectra has been normalized by setting the pre-edge region equal to one. 1 ML Zn-TPP results from Ref. [14] are added for comparison. Red (black) lines refer to spectra acquired with *s*(*p*)-polarized light.

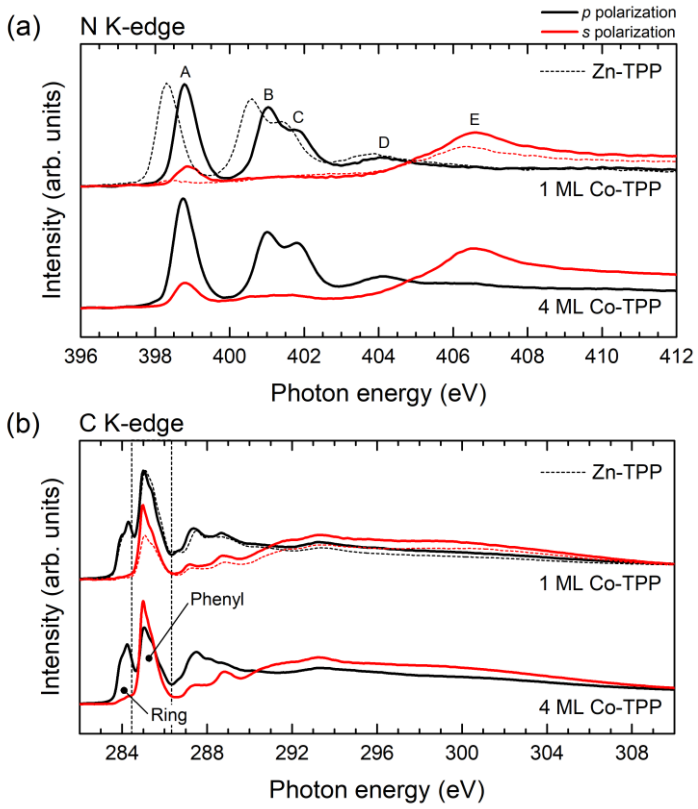


**Figure 6.** NEXAFS spectra acquired at the N (panel a) and C (panel b) K-edges on Co-TPP/Fe(001)-*p*(1×1)O. Dashed lines: 1 ML Zn-TPP on the same substrate; the shift of N K-edge adsorption features from the Zn-TPP layer with respect to the Co-TPP ones is consistent with the theoretical prediction of Ref. [48]. Red (black) lines refer to spectra acquired with *s*(*p*)-polarized light. Spectra from different coverages have been rescaled for a better comparison.

The N K-edge is characterized by four main peaks at 398.8, 401, 402 and 404 eV (labeled A, B, C and D in **Figure 6**a) below the ionization threshold, and one broad peak above it at 406.5 eV (labeled E). This is a characteristic shape of metalated porphyrins, where the different choice of the metal center mostly affects the energy position and relative weight of the main peaks, as can be appreciated by the comparison with spectra measured for Zn-TPP (shown in **Figure 6**a with dashed lines). The leading resonance A stems from transition from the N 1*s* to the LUMO, which has a dominant $\pi^*$-symmetry character, while all the other resonances result from a superposition of multiple transitions to higher order unoccupied orbitals (LUMO+i). When measured in *p*- and *s*-polarization, peaks A, B, C and D display an opposite dichroism with respect to peak E. In particular, peaks A, B, C and D are related to the excitation of

N 1*s* electrons into π*-symmetry molecular orbitals located on the tetra-pyrrole ring, while peak E displays a σ*-symmetry character. According to selection rules for *s*→*p* transitions, X-ray adsorption is promoted when the light polarization is perpendicular to the nodal plane of the related unoccupied orbital. In the case of a flat-lying aromatic molecule, for instance, no transitions into π*-symmetry orbitals are expected with *s*-polarized light.

By inspecting the spectra related to 1 ML Co-TPP in **Figure 6**a, it is possible to observe a clear discrepancy between the dichroism of peak A (LUMO) and that of the doublet B, C (LUMO+i). The latter displays a strong dichroism, indicative of a flat-lying tetra-pyrrole ring. This is consistent with the morphology observed with STM (**Figure 2**), showing molecules lying flat on the substrate. We ascribe the very small residual intensity in *s*-polarization (doublet B, C) to a local distortion of the tetra-pyrrole ring (*e.g.* an inflection, as reported for both metal [49] and oxide [50] substrates), rather than to a tilting of the entire ring with respect to the Fe surface. The larger intensity observed with *s*-polarized light in the position of the LUMO peak can be linked to a transition into a σ*-symmetry orbital, rather than the π*-symmetry state contributing to A peak in *p*-polarization. Such an additional resonance has been already reported for Co-phthalocyanine [51] as well as other metal porphyrins [47] and phthalocyanines, [25,52] which share the same electronic configuration of the macrocycle.[53] Detailed calculations for the case of Cu-TPP have shown that this σ*-symmetry resonance is associated with the transition from N 1*s* to the mixed N $2p_{x,y}$ - Metal $3d_{x^2-y^2}$ orbital.[53] The exact energy of this resonance is finally determined by the specific metal center [54] and the degree of interaction with the substrate.[55]

Similar to the results of our previous work on the Zn-TPP/Fe(001)-*p*(1 × 1)O system [14], the increased thickness of the Co-TPP film is reflected in a change of the intensity ratio of the B/C doublet peaks and in an increase of their contribution to the *s*-polarization signal. The latter observation can be attributed to the tilting of the entire

macrocycle with respect to the Fe surface, in agreement with the more disordered nature of the multilayer film.

The analysis of the C K-edge spectra of **Figure 6**b can be separated in two parts. First, the NEXAFS resonances at about 284 eV are associated exclusively with the π*-symmetry LUMO states localized on the tetra-pyrrole ring. As expected, they display a large dichroism with a very small residual intensity in *s*-polarization, in full agreement with that observed at the N K-edge on the purely π*-symmetry B, C, D resonances. Second, the large resonance at about 285 eV is mostly contributed by the transition to the π*-symmetry LUMO of the peripheral phenyl rings. The change of their linear dichroism signal moving from 1 ML to the multilayer film is associated to: (i) the rotation of the phenyl groups, from more bent towards the substrate to perpendicular to it, and (ii) a general increase of the degree of disorder of the molecular layer.

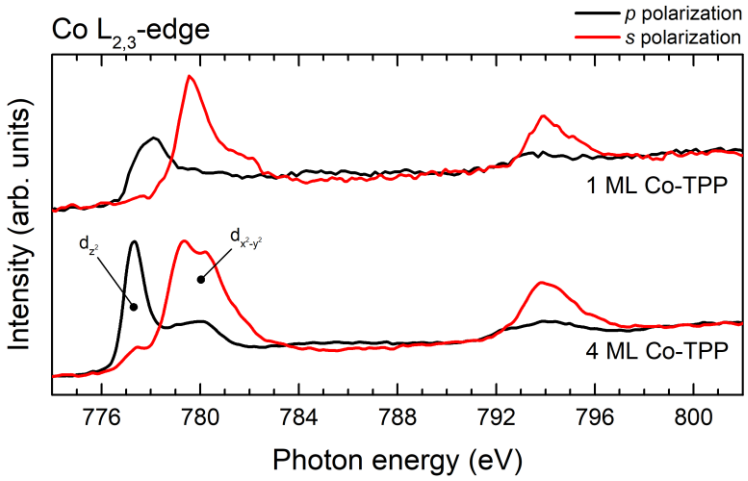


**Figure 7.** NEXAFS spectra acquired at the Co $L_{2,3}$ edges on Co-TPP/Fe(001)-*p*(1 × 1)O for different molecular coverages. Red (black) lines refer to spectra acquired with *s*(*p*)-polarized light. Spectra from different coverages have been rescaled for a better comparison.

**Figure 7** shows the NEXAFS spectra acquired at the Co $L_{2,3}$ edges. The interpretation of the results in terms of on selection rules is not as straightforward as with the N and C edges. However, analogies are noted with the work of Ref. [51] on Co phthalocyanines on Au(110). There, peak attribution is based on the $D_{4h}$ splitting

of 3*d* orbitals. The peak at about 777.3 eV (*p*-polarization) is likely to be related to adsorption into the empty $a_{1g}$ state with $d_{z^2}$ character, while the states at about 780 eV seen with *s*-polarization are probably due to adsorption into $b_{1g}$ states with $d_{x^2-y^2}$ character. The modification of the $d_{z^2}$ peak observed between 1 ML and 4 ML Co-TPP is indicative of charge redistribution in the direction perpendicular to the tetra-pyrrole ring, consistent with the UPS and XPS results of Section 3.2.

### 3.4 *First-principles calculations*

The molecular overlayer constitutes a square lattice with the lattice parameter equal to 5 iron lattice constants ($a_{\mathrm{Fe}} = 2.87$ Å), as deduced from the LEED analysis (see Section 3.1). The quasi-square shape of the TPP molecules can rotate of an azimuthal angle ($\alpha$, referred to the overlayer lattice vector) to reduce the steric hindrance among neighboring phenyl rings (see for example the case of Zn-TPP on the same surface [14]). Since the Co-TPP molecular lattice is not collinear with the substrate directions (LEED pattern in **Figure 1**), the rotation of the molecules by an angle of $\pm\alpha$ yields two non-equivalent configurations. We have considered these two rotations, optimizing for each of them the molecular coordinates and centering the Co atom on top of a Fe atom or an O one (4 total combinations). 2 are the most stable structures (see **Figure 8**), consisting in the molecular adsorption on either the Fe site (case A) or the O site (case B) but with opposite azimuthal orientations. These structures are nearly isoenergetic, with a difference below 0.02 eV. However, this fact does not imply a completely shallow interaction with the substrate being the other two combinations at least 0.2 eV higher in energy.

Of the two most stable configurations, we report structural details. A and B cases sizably differ by the azimuthal orientation with respect to the substrate. This can be seen by comparing the angle $\varphi$ formed between the [100] direction (black line in **Figure 8**) and the yellow line connecting the N atoms of the two pyrrole groups bent towards the surface. We found $\varphi$ = 55° and 20° for adsorption over the Fe site ($\varphi_{\mathrm{A}}$) and

O site ($\varphi_B$), respectively, which corresponds to angle $\alpha_A = \varphi_A - \theta = 18\,°$ and $\alpha_B = \varphi_B - \theta = -17\,°$, where $\theta$ is equal to 37 ° (see the Introduction). Hence, looking only to the molecular coordinates, the two A and B cases depicted in **Figure 8** are approximately equivalent through reflection across a mirror plane containing an overlayer lattice vector and the surface normal. As expected, the structural parameters are similar. In both cases, a significant distortion of the molecule with respect to the gas phase is found. In particular, adsorption enhances the saddle shape of the molecule, with two pyrrole rings approaching the surface with a tilt angle of 14.5° (case A) and 12.7° (case B) from the surface plane. The other two pyrrole rings tilt away from the surface by an angle of 20.1° (case A) and 21.7° (case B). This enhanced saddle-shape conformation of the macrocycle is in good agreement with the effective tilt angle drawn from the NEXAFS dichroism of the N K-edge B, C doublet and the C K-edge LUMO resonances (see **Figure 6**). This distortion facilitates the rotation of the plane of the phenyl rings towards the Fe surface, showing a final angle $\beta$ of 33.5° (case A) and 32.8° (case B) with respect to the substrate normal ($\beta = 69.0\,°$ is obtained for the free molecule).

Regarding the tetra-pyrrole ring, the inner Co atom sits 3.28 Å (case A) and 3.18 Å (case B) from the O layer.

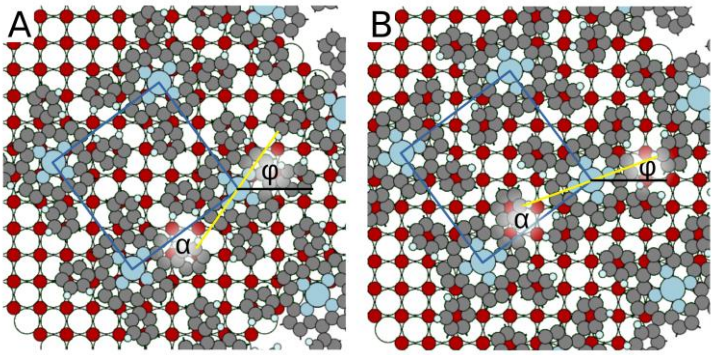


**Figure 8.** Top view of adsorption models for Co-TPP in the two azimuthal orientations, see the angle α between the yellow line (passing through N atoms of the pyrroles bent towards the surface) and the overlayer lattice vectors. Molecules are shown on their corresponding most stable adsorption site: on a Fe atom (left, case A) and on an O one (right, case B). The angle formed by the molecules with a crystal high-symmetry direction (black line) is indicated by $\varphi$. Gray, cyan, red, white circles mark C, N, O, and Fe atoms, respectively. The largest circle is for Co. Smallest circles are for the most-protruding H atoms (the others not shown).

In **Figure 9**, the simulated STM image of the adsorbed molecules is reported. The result has been computed in the Tersoff-Hamann approximation [56], *i.e.*, with an integration of the local density of states (LDOS) from the Fermi energy to the applied bias. By deriving a constant-LDOS isosurface, smeared by a Gaussian broadening of 1Å, the image contrast may enhance different part of the molecule (such as the central Co atom, the phenyl or the protruding pyrrole rings) depending on the specific tunneling conditions. As a result, STM maps can display both the two-fold symmetry previously observed for Zn-TPP on the same surface [14] and the four-fold geometry shown in this work. Co-TPP on a Fe site yields to a slightly better geometrical agreement with the STM image (see **Figure 2**) considering the orientation of the phenyl rings with respect to substrate directions.

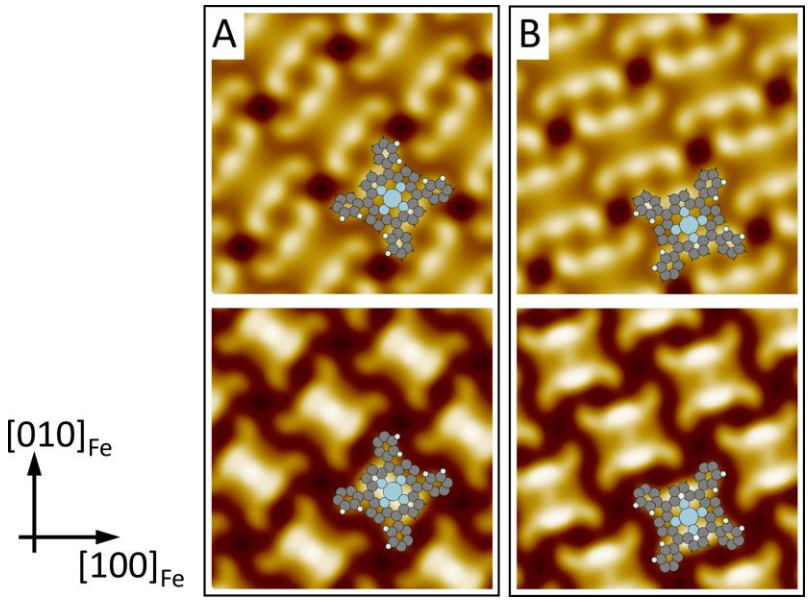


**Figure 9.** Simulated STM image for Co-TPP adsorbed at a Fe site (left column, case A) and at an O one (right column, case B). The applied bias varies from -2 eV (filled states, top row) to +2 eV (empty states, bottom row).

Qualitative information about the electronic properties of the interface can be gained by the analysis of the projected density of states (PDOS). In fact, a full agreement with experiments cannot be expected on the basis of the bare Kohn-Sham

results [57], the former requiring the inclusion of many-body correlations beyond the "+U" correction. Unfortunately, this approach becomes unpractical for this system size. We report in **Figure 10** the PDOS for Co-TPP on the Fe site, resolved into the two spin components and into the contributions by the substrate and the molecule (Co atom and the remaining C, N, and H ones). Regarding the molecular orbitals, features associated to states located in the tetra-pyrrole ring (R) are closer to the Fermi energy, then the electronic states derived from phenyl (Ph) localized orbitals follow. At even higher binding energies, the PDOS is characterized by less intense tetra-pyrrole ring states and a sharp peak due to phenyl atoms (see the feature at -4 eV). This reproduces the sequence found by UPS, even if with a significant energy scale compression, as expected from Kohn-Sham DFT.

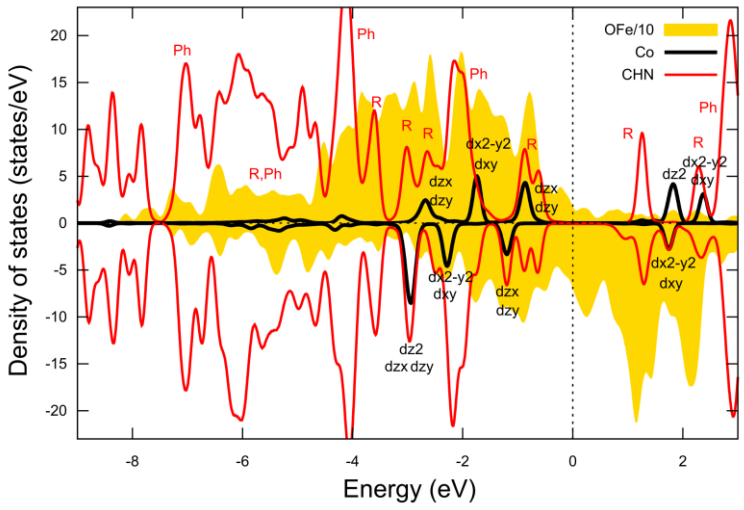


**Figure 10.** Computed density of states of Co-TPP/Fe(001)-*p*(1 × 1)O adsorbed above a Fe atom. The DOS for the spin minority component is shown reversed. The shaded area marks the contribution by the substrate atoms; the black thick line the contribution by the Co atom and the red thin one by C, H, and N in the molecule. Black labels mark the symmetry of *d* states (*e.g.*, $d_{z^2}$) and red labels mark the location of molecular states over the phenyls (Ph) or the tetra-pyrrole ring (R).

## 4. Conclusions

Single- and multilayer films of Co-TPP on oxygen passivated Fe, namely the Fe(001)-*p*(1×1)O surface, are analyzed and the results are compared with those of our previous investigation on Zn-TPP films on the same substrate. Our results definitely prove that ultra-thin metal oxide layers help the stabilization of ordered molecular overlayers and preserve the electronic properties characteristic of quasi-free porphyrins at monolayer coverage. Notwithstanding the presence of the same peripheral phenyl groups, however, Co-TPP molecules show a different assembly and a different degree of interaction with the substrate, with the formation of interfacial states. We link these differences to the different physical-chemical characteristics of the inner metal atom, determining the geometrical configuration of the metal-containing tetra-pyrrole ring and tuning the molecular reactivity.

M-TPP growth onto an ultra-thin metal oxide layer thus shows itself as an optimal model system where to focus experimental and modeling efforts with the aim of ultimately driving the supramolecular assembling and stabilizing of specific intra-molecular mechanisms.

## References:


[1] D. Dolphin, R.H. Felton, Biochemical significance of porphyrin π cation radicals, Acc. Chem. Res. 7 (1974) 26–32. doi:10.1021/ar50073a005.

[2] D. Dolphin, ed., The Porphyrins, Elsevier, 1978. doi:10.1016/B978-0-12-220101-1.X5001-X.

[3] A. Verdini, P. Shinde, G.L. Montanari, S.T. Suran-Brunelli, M. Caputo, G. Di Santo, C.A. Pignedoli, L. Floreano, D. Passerone, A. Goldoni, Water Formation for the Metalation of Porphyrin Molecules on Oxidized Cu(111), Chem. - An Eur. J. 22 (2016) 14672–14677. doi:10.1002/chem.201602105.

[4] C. Guan, L. Li, D. Chen, Z. Gao, W. Sun, Thermal behavior and thermal decomposition study of porphyrin polymers containing different spacer groups, Thermochim. Acta. 413 (2004) 31–38. doi:10.1016/j.tca.2003.11.002.

[5] S.-F. Pop, R.-M. Ion, M.C. Corobea, V. Raditoiu, Spectral and thermal investigations of porphyrin and phthalocyanine nanomaterials, J. Optoelectron. Adv. Mater. 13 (2011) 906–911.

[6] J.M. Gottfried, Surface chemistry of porphyrins and phthalocyanines, Surf. Sci. Rep. 70 (2015) 259–379. doi:10.1016/j.surfrep.2015.04.001.

[7] M. Campione, E. Fumagalli, L. Raimondo, A. Monguzzi, F. Meinardi, A. Sassella, Control of π–π Interactions in Epitaxial Films of Platinum(II) Octaethyl Porphyrin, Chem. Mater. 23 (2011) 832–840. doi:10.1021/cm102139h.

[8] G. Bussetti, M. Campione, M. Riva, A. Picone, L. Raimondo, L. Ferraro, C. Hogan, M. Palummo, A. Brambilla, M. Finazzi, L. Duò, A. Sassella, F. Ciccacci, Stable Alignment of Tautomers at Room Temperature in Porphyrin 2D Layers, Adv. Funct. Mater. 24 (2014) 958–963. doi:10.1002/adfm.201301892.

[9] A. Saywell, J.K. Sprafke, L.J. Esdaile, A.J. Britton, A. Rienzo, H.L. Anderson, J.N. O'Shea, P.H. Beton, Conformation and Packing of Porphyrin Polymer Chains Deposited Using Electrospray on a Gold Surface, Angew. Chemie Int. Ed. 49 (2010) 9136–9139. doi:10.1002/anie.201004896.

[10] V.C. Zoldan, R. Faccio, C. Gao, A.A. Pasa, Coupling of Cobalt–Tetraphenylporphyrin Molecules to a Copper Nitride Layer, J. Phys. Chem. C. 117 (2013) 15984–15990. doi:10.1021/jp4013625.

[11] C. Wäckerlin, K. Tarafder, J. Girovsky, J. Nowakowski, T. Hählen, A. Shchyrba, D. Siewert, A. Kleibert, F. Nolting, P.M. Oppeneer, T.A. Jung, N. Ballav, Ammonia Coordination Introducing a Magnetic Moment in an On-Surface Low-

Spin Porphyrin, Angew. Chemie Int. Ed. 52 (2013) 4568–4571. doi:10.1002/anie.201208028.

[12] J. Miguel, C.F. Hermanns, M. Bernien, A. Krüger, W. Kuch, Reversible Manipulation of the Magnetic Coupling of Single Molecular Spins in Fe-Porphyrins to a Ferromagnetic Substrate, J. Phys. Chem. Lett. 2 (2011) 1455–1459. doi:10.1021/jz200489y.

[13] C. Castellarin-Cudia, P. Borghetti, G. Di Santo, M. Fanetti, R. Larciprete, C. Cepek, P. Vilmercati, L. Sangaletti, A. Verdini, A. Cossaro, L. Floreano, A. Morgante, A. Goldoni, Substrate Influence for the Zn-tetraphenyl-porphyrin Adsorption Geometry and the Interface-Induced Electron Transfer, Chem. Phys. Chem. 11 (2010) 2248–2255. doi:10.1002/cphc.201000017.

[14] A. Picone, D. Giannotti, A. Brambilla, G. Bussetti, A. Calloni, R. Yivlialin, M. Finazzi, L. Duò, F. Ciccacci, A. Goldoni, A. Verdini, L. Floreano, Local structure and morphological evolution of ZnTPP molecules grown on Fe(001)-*p*(1 × 1)O studied by STM and NEXAFS, Appl. Surf. Sci. 435 (2018) 841–847. doi:10.1016/j.apsusc.2017.11.128.

[15] M.B. Casu, A. Schöll, K.R. Bauchspiess, D. Hübner, T. Schmidt, C. Heske, E. Umbach, Nucleation in Organic Thin Film Growth: Perylene on $Al_2O_3/Ni_3Al(111)$, J. Phys. Chem. C. 113 (2009) 10990–10996. doi:10.1021/jp809497h.

[16] B.-E. Schuster, M.B. Casu, I. Biswas, A. Hinderhofer, A. Gerlach, F. Schreiber, T. Chassé, Role of the substrate in electronic structure, molecular orientation, and morphology of organic thin films: diindenoperylene on rutile $TiO_2(110)$, Phys. Chem. Chem. Phys. 11 (2009) 9000. doi:10.1039/b912790a.

[17] R. Bertacco, F. Ciccacci, Oxygen-induced enhancement of the spin-dependent effects in electron spectroscopies of Fe(001) Phys. Rev. B 59 (1999) 4207-4210. doi: 10.1103/PhysRevB.59.4207

[18] A. Picone, A. Brambilla, A. Calloni, L. Duò, M. Finazzi, F. Ciccacci, Oxygen-induced effects on the morphology of the Fe(001) surface in out-of-equilibrium conditions, Phys. Rev. B. 83 (2011) 235402. doi:10.1103/PhysRevB.83.235402.

[19] R. Bertacco, F. Ciccacci, Oxygen-induced enhancement of the spin-dependent effects in electron spectroscopies of Fe(001), Phys. Rev. B. 59 (1999) 4207–4210. doi:10.1103/PhysRevB.59.4207.

[20] D.T. Pierce, R.J. Celotta, G. -C. Wang, W.N. Unertl, A. Galejs, C.E. Kuyatt, S.R. Mielczarek, The GaAs spin polarized electron source, Rev. Sci. Instrum. 51 (1980) 478–499. doi:10.1063/1.1136250.

[21] F. Ciccacci, G. Chiaia, Comparative study of the preparation of negative electron affinity GaAs photocathodes with $O_2$ and with $NF_3$, J. Vac. Sci. Technol. A Vacuum, Surfaces, Film. 9 (1991) 2991–2995. doi:10.1116/1.577161.

[22] F. Ciccacci, E. Vescovo, G. Chiaia, S. De Rossi, M. Tosca, Spin-polarized electron gun for electron spectroscopies, Rev. Sci. Instrum. 63 (1992) 3333–3338. doi:10.1063/1.1142549.

[23] M. Finazzi, A. Bastianon, G. Chiaia, F. Ciccacci, High-sensitivity bandpass UV photon detector for inverse photoemission, Meas. Sci. Technol. 4 (1993) 234–236. doi:10.1088/0957-0233/4/2/017.

[24] G. Chiaia, S. De Rossi, L. Mazzolari, F. Ciccacci, Thin Fe films grown on Ag(100) studied by angle- and spin-resolved inverse-photoemission spectroscopy, Phys. Rev. B. 48 (1993) 11298–11304. doi:10.1103/PhysRevB.48.11298.

[25] L. Floreano, A. Cossaro, R. Gotter, A. Verdini, G. Bavdek, F. Evangelista, A. Ruocco, A. Morgante, D. Cvetko, Periodic Arrays of Cu-Phthalocyanine Chains on Au(110), J. Phys. Chem. C. 112 (2008) 10794–10802. doi:10.1021/jp711140e.

[26] T. Thonhauser, S. Zuluaga, C. A. Arter, K. Berland, E. Schröder, P. Hyldgaard, Spin Signature of Nonlocal Correlation Binding in Metal-Organic Frameworks, Phys. Rev. Lett. 115 (2015) 136402. doi: 10.1103/PhysRevLett.115.136402.

[27] P. Giannozzi, S. Baroni, N. Bonini, M. Calandra, R. Car, C. Cavazzoni, D. Ceresoli *et al.*, QUANTUM ESPRESSO: a modular and open-source software project for quantum simulations of materials, J. Phys.: Condens. Matter 21 (2009) 395502. doi: 10.1088/0953-8984/21/39/395502.

[28] P. Giannozzi, O. Andreussi, T. Brumme, O. Bunau, M. Buongiorno Nardelli, M. Calandra, R. Car *et al.*, Advanced capabilities for materials modelling with Quantum ESPRESSO, J Phys.: Condensed Matter 29 (2017) 465901. doi:10.1088/1361-648X/aa8f79.

[29] A. Picone, G. Fratesi, A. Brambilla, P. Sessi, F. Donati, S. Achilli, L. Maini, M. I. Trioni, C. S. Casari *et al.*, Atomic corrugation in scanning tunneling microscopy images of the Fe(001)-$p(1 \times 1)$, Phys. Rev. B 81 (2010) 115450. doi: 10.1103/PhysRevB.81.115450.

[30] H. J. Monkhorst, J. D. Pack, Special points for Brillouin-zone integrations, Phys. Rev. B 13 (1976) 5188-5192. doi:10.1103/PhysRevB.13.5188.

[31] A. M. Ritzmann, M. Pavone, A. B. Muñoz-García, J. A. Keith, E. A. Carter, Ab initio DFT+U analysis of oxygen transport in $LaCoO_3$: the effect of $Co^{3+}$ magnetic states, J. Mater. Chem. A 2 (2014) 8060-8074. doi:10.1039/c4ta00801d.

[32] S.-J. Hu, S.-S. Yan, M.-W. Zhao, L.-M. Mei, First-principles LDA+U calculations of the Co-doped ZnO magnetic semiconductor, Phys. Rev. B, 73 (2006) 245205. doi:10.1103/PhysRevB.73.245205.

[33] K. Leung, S. B. Rempe, P. A. Schultz, E. M. Sproviero, V. S. Batista, M. E. Chandross, C. J. Medforth, Density Functional Theory and DFT+U Study of

Transition Metal Porphines Adsorbed on Au(111) Surfaces and Effects of Applied Electric Fields, JACS 11 (2006) 3659-3668. doi:10.1021/ja056630o.

[34] M.-S. Liao, S. Scheiner, Electronic structure and bonding in metal porphyrins, metal = Fe, Co, Ni, Cu, Zn, J. Chem. Phys. 117 (2002) 205-219. doi:10.1063/1.1480872.

[35] K. Hermann, M.A. Van Hove, LEEDpat4 (LEED pattern analyzer), (2015). http://www.fhi-berlin.mpg.de/KHsoftware/LEEDpat/.

[36] G. Bussetti, A. Calloni, M. Celeri, R. Yivlialin, M. Finazzi, F. Bottegoni, L. Duò, F. Ciccacci, Structure and electronic properties of Zn-tetra-phenyl-porphyrin single- and multi-layers films grown on Fe(001)- p (1 × 1)O, Appl. Surf. Sci. 390 (2016) 856–862. doi:10.1016/j.apsusc.2016.08.137.

[37] S. Rangan, S. Katalinic, R. Thorpe, R.A. Bartynski, J. Rochford, E. Galoppini, Energy Level Alignment of a Zinc(II) Tetraphenylporphyrin Dye Adsorbed onto TiO2(110) and ZnO(11$\bar{2}$0) Surfaces, J. Phys. Chem. C. 114 (2010) 1139–1147. doi:10.1021/jp909320f.

[38] S.C. Khandelwal, J.L. Roebber, The photoelectron spectra of tetraphenylporphine and some metallo tetraphenylporphyrins, Chem. Phys. Lett. 34 (1975) 355–359. doi:10.1016/0009-2614(75)85292-4.

[39] L. Scudiero, D.E. Barlow, U. Mazur, K.W. Hipps, Scanning Tunneling Microscopy, Orbital-Mediated Tunneling Spectroscopy, and Ultraviolet Photoelectron Spectroscopy of Metal(II) Tetraphenylporphyrins Deposited from Vapor, J. Am. Chem. Soc. 123 (2001) 4073–4080. doi:10.1021/ja0100726.

[40] T. Lukasczyk, K. Flechtner, L.R. Merte, N. Jux, F. Maier, J.M. Gottfried, H.-P. Steinrück, Interaction of Cobalt(II) Tetraarylporphyrins with a Ag(111) Surface Studied with Photoelectron Spectroscopy, J. Phys. Chem. C. 111 (2007) 3090–3098. doi:10.1021/jp0652345.

[41] T. Kroll, R. Kraus, R. Schönfelder, V.Y. Aristov, O. V. Molodtsova, P. Hoffmann, M. Knupfer, Transition metal phthalocyanines: Insight into the electronic structure from soft x-ray spectroscopy, J. Chem. Phys. 137 (2012) 054306. doi:10.1063/1.4738754.

[42] W. Hieringer, K. Flechtner, A. Kretschmann, K. Seufert, W. Auwärter, J. V. Barth, A. Görling, H.-P. Steinrück, J.M. Gottfried, The Surface Trans Effect: Influence of Axial Ligands on the Surface Chemical Bonds of Adsorbed Metalloporphyrins, J. Am. Chem. Soc. 133 (2011) 6206–6222. doi:10.1021/ja1093502.

[43] A. Picone, D. Giannotti, M. Riva, A. Calloni, G. Bussetti, G. Berti, L. Duò, F. Ciccacci, M. Finazzi, A. Brambilla, Controlling the Electronic and Structural Coupling of C 60 Nano Films on Fe(001) through Oxygen Adsorption at the Interface, ACS Appl. Mater. Interfaces. 8 (2016) 26418–26424. doi:10.1021/acsami.6b09641.

[44] S.D. Pop, S.P. Kate, J. Rappich, K. Hinrichs, Tunable optical constants of thermally grown thin porphyrin films on silicon for photovoltaic applications, Sol. Energy Mater. Sol. Cells. 127 (2014) 169–173. doi:10.1016/j.solmat.2014.04.032.

[45] M. Knupfer, Exciton binding energies in organic semiconductors, Appl. Phys. A. 77 (2003) 623-626. doi:10.1007/s00339-003-2182-9.

[46] C.D. Wagner, W.M. Riggs, L.E. Davis, J.F. Moulder, G.E. Muilenberg, Handbook of X-Ray Photoelectron Spectroscopy, Perkin- Elmer Corporation, Physical Electronics Division, Eden Prairie, MN, 1979.

[47] G. Zamborlini, M. Jugovac, A. Cossaro, A. Verdini, L. Floreano, D. Lüftner, P. Puschnig, V. Feyer, C. M. Schneider, On-surface nickel porphyrin mimics the reactive center of an enzyme cofactor, Chem. Comm. 54 (2018) 13423. doi:10.1039/C8CC06739B.

[48] N. Schmidt, R. Fink, W. Hieringer, Assignment of near-edge x-ray absorption fine structure spectra of metalloporphyrins by means of time-dependent density-functional calculations, J. Chem. Phys. 133 (2010) 054703. doi:10.1063/1.3435349.

[49] D. Wechsler, M. Franke, Q. Tariq, L. Zhang, T.-L. Lee, P.K. Thakur, N. Tsud, S. Bercha, K.C. Prince, H.-P. Steinrück, O. Lytken, Adsorption Structure of Cobalt Tetraphenylporphyrin on Ag(100), J. Phys. Chem. C. 121 (2017) 5667–5674. doi:10.1021/acs.jpcc.7b00518.

[50] G. Lovat, D. Forrer, M. Abadia, M. Dominguez, M. Casarin, C. Rogero, A. Vittadini, L. Floreano, Very high temperature tiling of tetraphenylporphyrin on rutile $TiO_2$(110), Nanoscale 9 (2017) 11694-11704. doi:10.1039/C7NR04093H.

[51] M.G. Betti, P. Gargiani, R. Frisenda, R. Biagi, A. Cossaro, A. Verdini, L. Floreano, C. Mariani, Localized and Dispersive Electronic States at Ordered FePc and CoPc Chains on Au(110), J. Phys. Chem. C. 114 (2010) 21638–21644. doi:10.1021/jp108734u.

[52] D. G. De Oteyza, A. Sakko, A. El-Sayed, E. Goiri, L. Floreano, A. Cossaro, J. M. Garcia-Lastra, A. Rubio, J. E. Ortega, Inversed linear dichroism in F K-edge NEXAFS spectra of fluorinated planar aromatic molecules, Phys. Rev. B 86 (2012) 075469. doi:10.1103/PhysRevB.86.075469.

[53] G. Mangione, M. Sambi, S. Carlotto, A. Vittadini, G. Ligorio, M. Timpel, L. Pasquali, A. Giglia, M. V. Nardi, M. Casarin, Electronic structure of CuTPP and CuTPP(F) complexes: a combined experimental and theoretical study II, Phys. Chem. Chem. Phys. 18 (2016) 24890-24904. doi:10.1039/C6CP03956A.

[54] R. De Francesco, M. Stener, G. Fronzoni, Theoretical Study of Near-Edge X-ray Absorption Fine Structure Spectra of Metal Phthalocyanines at C and N K-Edges, J. Phys. Chem. A 116 (2012) 2885-2894. doi:10.1021/jp2109913.

[55] M. V. Nardi, F. Detto, L. Aversa, R. Verucchi, G. Salviati, S. Iannotta, M. Casarin, Electronic properties of CuPc and $H_2Pc$: an experimental and theoretical study, Phys. Chem. Chem. Phys. 15 (2013) 12864-12881. doi:10.1039/c3cp51224j.

[56] J. Tersoff, D. R. Hamann, Theory of the scanning tunneling microscope, Phys. Rev. B 31 (1985) 805-813. doi: 10.1103/PhysRevB.31.805.

[57] X. Blase, C. Attaccalite, V. Olevano, First-principles *GW* calculations for fullerenes, porphyrins, phtalocyanine, and other molecules of interest for organic photovoltaic applications, Phys. Rev. B 83 (2011) 115103. doi:10.1103/PhysRevB.83.115103.